A Free-Surface Model of a Jet Impinging On a Sprinkler Head

TAYLOR MYERS[1], ANDRÉ MARSHALL[1], and HOWARD BAUM[1]
[1]University of Maryland, College Park

ABSTRACT Understanding the atomization of fire sprinkler sprays fills a critical gap in the modeling of fire suppression systems. Previous research by the authors has shown an instability model coupled with a stochastic transport model can paint most of the sprinkler spray picture, but requires input in the form of thickness and velocity of unstable fluid sheets. The model outlined describes a water jet impinging on a perforated deflector plate as a velocity potential. The free surface separating the jet from the surrounding air takes the form of a vortex sheet with the air assumed to be at rest. Through the use of the Green's function, the fluid velocity potential can be posed as a boundary value problem. Any solution obtained is an exact solution to the inviscid flow equations and the interior flow a solution to the Navier-Stokes equations. The resulting model allows for the determination of the complete flow field over a sprinkler head of arbitrary geometry and input conditions. Knowledge of this flow field provides insight into the impact of sprinkler head geometry and fluid velocity as well as providing the above mentioned inputs for a complete model of fire sprinkler sprays.

KEYWORDS: suppression, fluid dynamics, CFD

NOMENCLATURE LISTING

A_s	area of deflector plate openings (m^2)
f	free-surface location
G	Green's function
J_0	Bessel function of order zero
$\mathcal{G}$	axisymmetric Green's function
p	pressure of fluid (Pa)
p_s	static pressure of fluid (Pa)
R_j	radius of jet boundary (m)
R_s	radius of the centroid of the slot (m)
R_{ts}	arbitrary radius of tine stream boundary (m)
$\vec{r}$	spatial location (m)
$\vec{r}_0$	source location (m)
r	radial spatial location (m)
r_0	radial source location (m)
U_j	jet velocity (m/s)
u	radial velocity (m/s)
v	vertical velocity (m/s)
Z_j	arbitrary height of jet boundary (m)
z	vertical spatial location (m)
z_0	vertical source location (m)
z_s	tine sheet thickness (m)

Greek

α	flow split
δ	Dirac Delta function
λ_n	Eigenvalue of the order zero Bessel function
θ	angular spatial location
ρ	fluid density (kg/m^3)
Φ	perturbation potential
ϕ	fluid potential

INTRODUCTION

Sprinkler systems are a ubiquitous form of fire protection in the United States with expanding adoption around the world. The performance of a sprinkler depends on the spray generated by the sprinkler, the dispersion of the spray within the flames, and the wetting of burning surfaces. Despite the widespread use of sprinklers, analytical models to predict their performance have yet to be developed. Each one of these stages of sprinkler modeling involve complex transport processes which create important modeling and measurement challenges. The transport processes responsible for sprinkler performance are complex, not readily yielding to measurement or analysis, making the development of analytical models difficult.

The possibility of accurately predicting water delivery with fire models, or more ambitiously, of designing sprinklers with models to produce particular sprays, has far reaching implications for suppression technology and engineering practices. The goal of the present paper is to introduce a general scheme for predicting sheet formation from the impingement of a jet onto a deflector, a configuration common to most sprinklers. This scheme provides insight into how deflectors govern sprinkler spray behavior and represents an important fundamental sub-model required for predicting the initial sprinkler spray.

The atomization mechanisms responsible for sprinkler spray formation are both unstable and chaotic. Though diverse in size, shape, and design details, most modern fire sprinklers use the same fundamental impinging jet configuration for spray generation illustrated in Fig. 1. In this configuration, water is initially forced through an orifice to produce a continuous water jet. This jet then impinges onto a deflector to form thin sheets of water (described by the modeling scheme developed in the current study). These thin, unstable sheets then disintegrate into ligaments, which, in turn, break into droplets [1].

There are multiple well-explored methods available to predict the droplet formation. For example, scaling laws have been developed which characterize droplet breakup locations as well as drop sizes in terms of sprinkler geometry, ambient conditions, and liquid flow properties [2, 3]. Alternatively, more detailed linear stability models describing the growth of the disturbances (i.e. sinusoidal waves) responsible for breakup are also available. In both cases, explicitly in the former and implicitly in the latter, sheet thickness and velocity are fundamental to the equations describing sprinkler spray characteristics. The determination of this sheet is thus very important to the overall characterization of the sprinkler spray.

In typical fire sprinklers, sheets are formed as the jet is turned along the deflector tines and as the jet is forced through the deflector slots as shown in Fig. 1. In order to predict the thickness and velocity of these sheets, one must have an understanding of the sprinkler-head flow responsible for their formation. The essential challenge in modeling sprinkler-head-fluid interactions is resolving the free-surface interface between liquid-phase water and gas-phase ambient air. This boundary-defined interface creates extremely thin sheets making the determination of its precise location critically important. In a preliminarry study to address the challenge of locating the liquid-gas interface (and the associated sheet thickness and velocity), the Volume of Fluid (VOF) method as outlined in Hirt [4] was applied to a sprinkler-head simulation. The VOF method is a simple but powerful approach designed with the goal of tracking the shape and position of the interface during multi-phase computational fluid dynamics (CFD) simulations. However, the computational burden to calculate the gas flow, liquid flow, and their interactions during the CFD based sprinkler-head simulation was prohibitive owing to mesh requirements for resolution of the thin sheets (with typical grid sizes of tens of microns) formed by the deflector (with typical sizes of tens of millimeters).

A new and more efficient alternative formulation for the sprinkler-head deflector flow problem is posed based on free-streamline flow theory. A free surface describes the surface of a fluid that is subject to constant perpendicular normal stress. The boundary between two homogeneous fluids; in this case, the impinging water jet and the surrounding air, can be described as a constant pressure free surface. Because of this constant pressure free-surface description of the jet, it is known that there is no flow normal to the jet boundary and thus the liquid-air boundary is a free streamline. The essential notion is to make use of the fact that a free-surface model of the flow can be constructed based on the description of the water jet as a velocity potential. Using the potential flow assumptions, the fluid velocity potential solutions can be reduced to a boundary value problem. Recognizing the velocity potential satisfies Laplace's equation and that the velocity potential may be specified on all boundaries, a complete velocity potential field within the boundaries may be realized along with the shape of the free-surface boundary itself.

This formulation removes the need to solve the Navier-Stokes equations for the water and the air on the volume surrounding the deflector for determination of the water-air interface. Figure 2a shows that in a traditional CFD approach tremendously detailed gridding is required to resolve the thin sheets (on the order of 50 microns). In contrast, in the free-surface modeling approach as shown in Fig. 2b, only the boundaries of the liquid stream require solution, greatly reducing computational requirements, typcially by about a factor of 100.

The mathematical formulation of this model is discussed next.

MATHEMATICAL MODEL

There is considerable literature describing two-dimensional free streamline flows dating back to the late nineteenth century. These problems have typically been addressed using the hodograph method, which uses the velocity components as independent variables [5, 6]. These flows are typically characterized by solid bound-

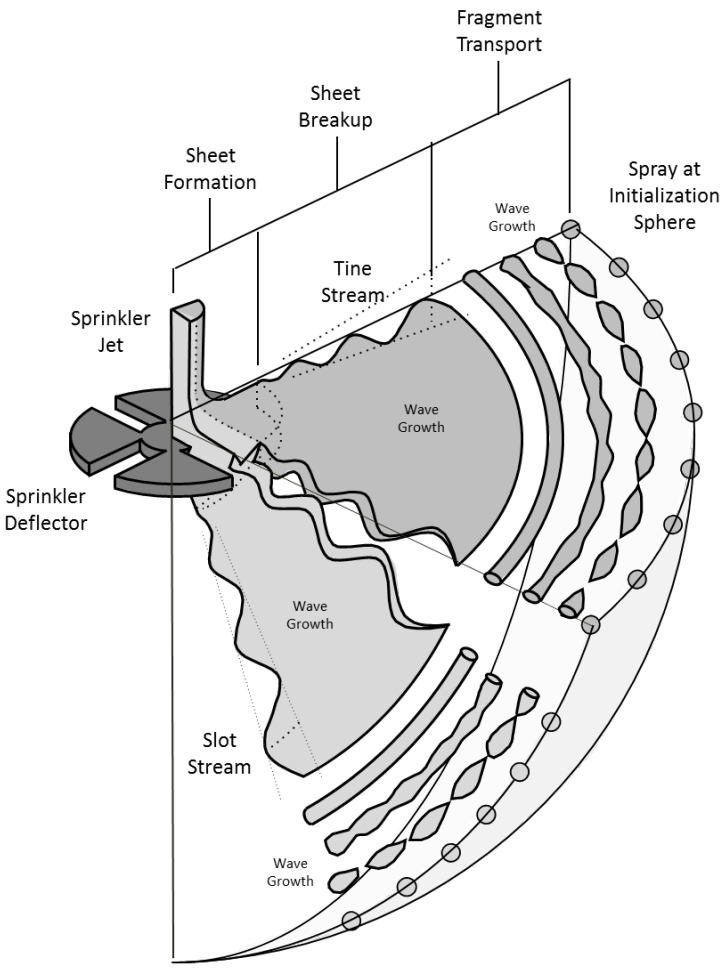

Fig. 1. An illustration of a three part model for sprinkler patternation and droplet formation.

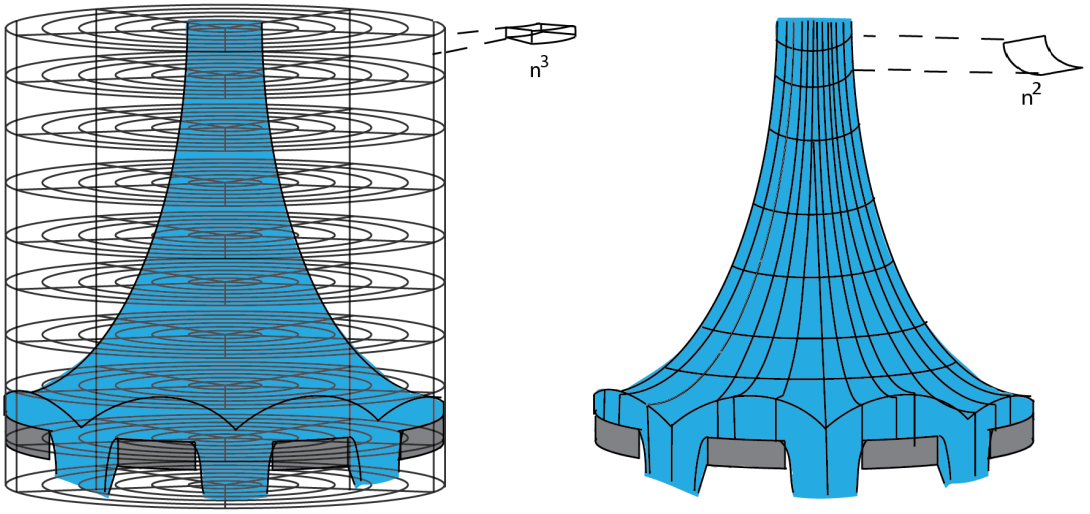

Fig. 2. Dimension and gridding requirements for deflector flow simulations in (a) traditional computational fluid dynamics approach and (b) the proposed boundary value problem approach.

aries composed of straight-line segments with the free surface being a streamline at a constant pressure. These qualities make determination of the boundary shape in the hodograph plane straightforward. Further, the fact that the velocity components are functions of a complex variable makes conformal mapping a powerful tool in constructing the solution.

In three dimensions the hodograph method is no longer available, nor is the use of complex variable techniques. However, the potential flow still satisfies the Laplace's equation and the free streamline remains a constant pressure surface. The free streamlines separating the water jet from the surrounding air are taken to be vortex sheets and the air is assumed to be at rest. The method relies on the existance of a Green's function satisfying the potential flow equation and appropriate boundary and symmetry conditions. In mathematics, a Green's function is a specific type of function used to solve inhomogeneous differential equations. It is a function which transforms a boundary value of a function into the functions response to the boundary value across all space. Physically the Green's function may be thought of as a weighting function or a propagator function. $G(\vec{r},\vec{r}_0)$ gives the effect of a unit point source ar $\vec{r}_0$ producing a potential at $\vec{r}$.

The formulation of the boundary value problem in terms of an appropriate characteristic Green's function reduces the problem to the determination of the shape of the free surface and the outflow conditions on the deflector plate.The boundary conditions required for definition of the Green's functions are dictated by the description of the sprinkler geometry and the nature of the incoming flow.

The general nature of the model presented in this study provides the capability of capturing the critical sheet behavior for fire sprinklers of almost any design complexity. It shares the advantage of the VOF method in being able to precisely capture interface location as well as the ability of the CFD model to exactly model the fluid flow. Additionally, it achieves both of these goals with relatively minimal computational burden.

To begin development of the mathematical model, the problem is posed in cylindrical coordinates as follows. The spatial location is given as

$$\vec{r} = (x,y,z) = (r\cos(\theta), r\sin(\theta), z) \tag{1}$$

and a source location given as

$$\vec{r_0} = (x_0,y_0,z_0) = (r_0\cos(\theta_0), r_0\sin(\theta_0), z_0). \tag{2}$$

The starting point of the mathematical formulation is the assumption that, because of the size and speeds associated with sprinkler heads (on the order of 0.01 m and 10 m/s, respectively), the effects of gravity and boundary layers can be disregarded. We can than define an impinging jet velocity field, $\vec{u}(\vec{r})$, which can be described as a potential flow satisfying the equation

$$\nabla^2\phi(\vec{r}) = 0, \qquad \text{where} \qquad \vec{u}(\vec{r}) = \nabla\phi(\vec{r}). \tag{3}$$

Figure 3a shows the fluid potential of an axisymmetric jet impinging on solid plate. The velocity, $\vec{u}(\vec{r})$, is always perpendicular to the isocontours of $\phi(\vec{r})$. The local pressure change, $p - p_\infty$, is determined by the gravity free Bernoulli equation given by

$$\rho u^2/2 + p_s = constant = \rho U_j^2/2. \tag{4}$$

where U_j is the velocity of the impinging jet. Figure 3b shows the nondimensional pressure of the same axisymmetric jet, with potential depicted in Fig. 3a, calculated using the gravity free Bernoulli equation.

Having established these preliminaries the sprinkler boundary value problem can now be formulated. The Green's function is a solution to

$$\nabla^2 G(\vec{r},\vec{r}_0) = \delta(\vec{r} - \vec{r}_0). \tag{5}$$

Here δ denotes the Dirac Delta function in three spatial dimensions.

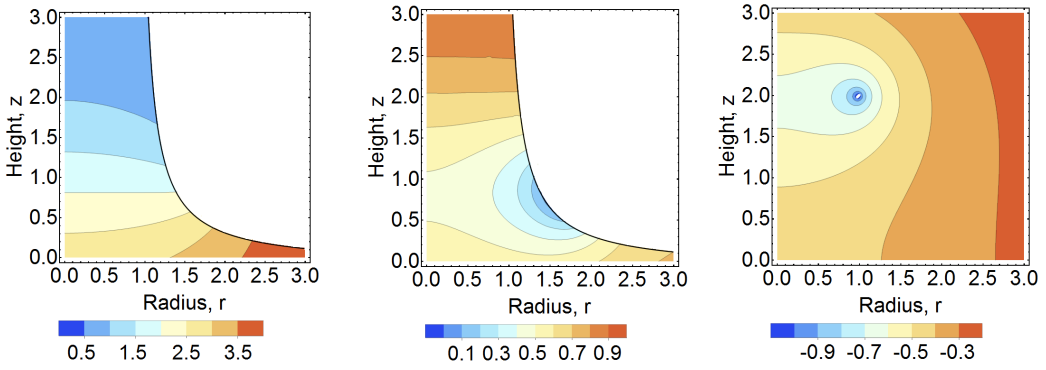

(a) (b) (c)

Fig. 3. For an axisymmetric jet impinging on a solid, horizontal plate the (a) fluid potential, $\phi(\vec{r})$, (b) static pressure, $p_s(\vec{r})$, and (c) the Green's function, $G_1(r,1,z,2)$

Next consider the integral $\phi(\vec{r})$ can be defined by

$$\phi(\vec{r}) = \int \phi(\vec{r}_0)\delta(\vec{r}-\vec{r}_0)\,d\vec{r}_0. \tag{6}$$

From Eqs. 3, 5, and 6, $\phi(\vec{r})$ can be defined as the integral

$$\phi(\vec{r}) = \int \left[\phi(\vec{r}_0)\nabla^2 G(\vec{r},\vec{r}_0) - \nabla^2\phi(\vec{r}_0)G(\vec{r},\vec{r}_0)\right] d^3\vec{r}_0 \tag{7}$$

The integral above is taken over the entire volume of the flow being solved. In the general case, this volume includes the jet bounded by the inlet, its free-surface, and the deflector that it impinges on. It is important to note that this formulation by itself assumes nothing about the geometry of the problem.

Second, $\phi(\vec{r})$ can be written in the form

$$\phi(\vec{r}) = \int \nabla\cdot\left[\phi(\vec{r}_0)\,\nabla G(\vec{r},\vec{r}_0) - \nabla\phi(\vec{r}_0)\,G(\vec{r},\vec{r}_0)\right] d^3\vec{r}_0. \tag{8}$$

Using the divergence theorem, the above can be rewritten as

$$\phi(\vec{r}) = \oint \left[\phi(\vec{r}_s)\,\frac{\partial G}{\partial n}(\vec{r},\vec{r}_s) - G(\vec{r},\vec{r}_s)\,\frac{\partial\phi}{\partial n}(\vec{r}_s)\right] d^2 s. \tag{9}$$

The integral in Eq. 9 is taken over the surface which bounds the volume of interest. Here, $\hat{n}$ is the local coordinate unit normal to the bounding surface pointing outward from the volume and $\vec{r}_s$ denotes point along that surface.

This result is very general and assumes nothing about the specific boundary conditions or the shape of the boundaries that are needed to obtain it. To proceed further it is necessary to specify the information available to formulate a specific boundary value problem relevant to the sprinkler jet impingement on a given deflector plate. The unknowns are, as mentioned above, the values of $\phi(\vec{r})$ along the boundaries, the fluid velocity, $u(\vec{r})$, normal to the boundaries, and a specific choice of a Green's function, $G(\vec{r},\vec{r}_0)$. The choice of Green's function will be considered next.

The starting point is the observation that the simplest Green's function satisfying Eq. 5, denoted here by $G_0(\vec{r}, r_o, \theta_o, z_o)$, is:

$$G_0(\vec{r}, r_o, \theta_o, z_o) = -\frac{1}{4\pi}\frac{1}{|\vec{r}-\vec{r}_0|} = -\frac{1}{4\pi}\frac{1}{\sqrt{r^2+r_o^2-2rr_o\cos(\theta-\theta_o)+(z-z_o)^2}}. \tag{10}$$

This solution satisfies Eq. 5, but is not particularly useful. There exist a variety of solutions to Eq. 5, all of which are acceptable Green's functions for use in the solution of Eq. 9. A simple modification can be made for the case of a planar barrier located at $z_0 = 0$, a reasonable approximation to a sprinkler deflector. The appropriate Green's function is then:

$$G_1(\vec{r}, r_o, \theta_o, z_o) = G_0(\vec{r}, r_o, \theta_o, z_o) + G_0(\vec{r}, r_o, \theta_o, -z_o). \tag{11}$$

The new solution still satisfies Eq. 5 and also satisfies the condition of no normal gradient at the surface $z_o = 0$. Figure 3c shows G_1 for a source located at $r_0 = 1$, $z_0 = 2$. Because the velocity component normal to the barrier either vanishes or is prescribed everywhere, the first term in Eq. 8 vanishes along the deflector boundary allowing the integral along the deflector boundary to be solved with only knowledge of the Green's function and the velocity normal to the deflector plate.

In this manner the Green's function can be further modified depending on the specific problem being considered. The particular choice of Green's function provides a limited amount of constraint to the problem. The remainder of the constraint will follow from the boundary conditions chosen and will reflect the geometry of the specific problem. In order to generally explore the impact of changing boundary conditions the major simplification of an axisymmetric flow pattern will be introduced in the following section.

AXISYMMETRIC MODEL

The full form of the boundary value problem is quite general and can be applied to complex boundary shapes.This complexity can make explaining the modeling approach difficult and obscure the impact of essential sprinkler geometric features. In an effort to provide insight into the impact of variations of the boundary conditions, as well as to clarify the general formulation of the boundary problem, a non-dimensional axisymmetric model will be demonstrated in this study.

Before proceeding to explore the boundary conditions, it is useful to introduce the dimensionless variables

$$\phi = U_j R_j \tilde{\phi}(\tilde{r}, \tilde{z}), \qquad \tilde{r} = r/R_j, \qquad \tilde{z} = z/R_j, \qquad \tilde{u} = \frac{\partial \tilde{\phi}}{\partial \tilde{r}}, \qquad \tilde{v} = \frac{\partial \tilde{\phi}}{\partial \tilde{z}}. \tag{12}$$

The tilde notation will be dropped for the remainder of the paper for the convenience of the vector notation. Owing to this non-dimensionalization $R_j = 1$ and $U_j = 1$.

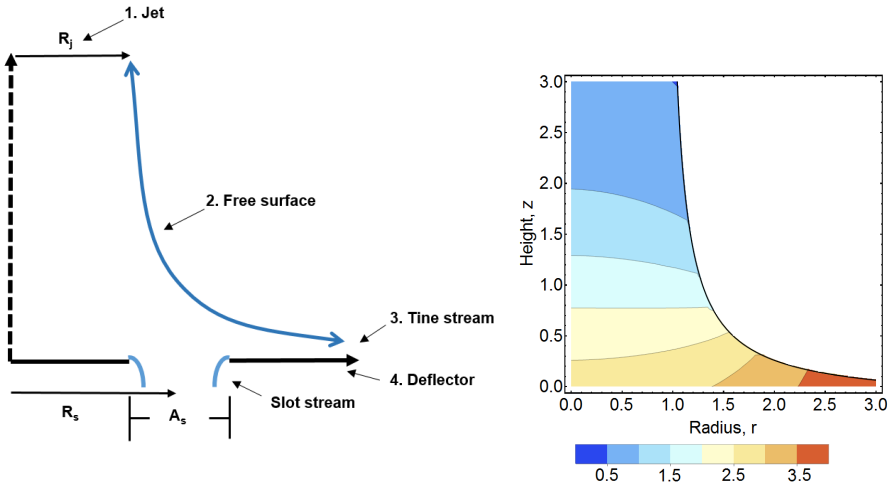

(a) (b)

Fig. 4. (a) The parameters of an axisymmetric model and (b) the potential flow field resulting from an axisymmetric deflector.

The axisymmetric model suggested here is posed as follows: an inviscid, vertical jet with radius R_j impinges upon a horizontal deflector plate. A ring opening with centroid R_s and total area A_s is located in the deflector plate. Here both slot centroid, R_s, and slot area, A_s, are non-dimensionalized by the impinging jet radius and area, R_j and πR_j^2, respectively. In a typical sprinkler head, slot penetrations in the deflector plate have some angular dependence. In the axisymmetric model suggested the discrete openings in the actual plate are smeared out uniformly with respect to the angular coordinate, θ, and the radial location and width of the smeared locations are chosen to match the last two parameters mentioned above. By assuming the flow pattern to be axially symmetric, some of the geometric effects induced by the details of the deflector plate geometry are lost, but the impact of the general geometry of slots is preserved. Figure 4a shows the definition of R_s and A_s for this general axisymmetric case.

The boundary conditions of $\phi(\vec{r}_s)$ and its normal gradient, $\hat{n}\cdot\nabla\phi(\vec{r}_s)$, appearing in Eq. 9, are independent of θ. All of the bounding surfaces are now figures of revolution, and the only quantities containing an angular dependence are the Green's function and its normal derivative. An axisymmetric Green's function can now be achieved by angularly integrating the Green's function presented in Eq. 10. The result takes the form

$$\mathcal{G}(\vec{r}, r_o, z_o) = -\frac{1}{4\pi}\int_0^{2\pi} \frac{1}{\sqrt{r^2 + r_o^2 - 2rr_o\cos(\theta-\theta_o)+(z-z_o)^2}}\, d\theta_o. \tag{13}$$

The quantity, $\mathcal{G}$, physically represents a ring source of fluid situated at $r = r_o$, $z = z_o$. The Green's function can then be rewritten as

$$\mathcal{G}(\vec{r}, r_o, z_o) = -\frac{1}{\pi\sqrt{(r+r_o)^2+(z-z_o)^2}}\int_0^{\pi/2}\left(1-\frac{4rr_o}{(r+r_o)^2+(z-z_o)^2}\sin^2(\theta)\right)^{-1/2} d\theta. \tag{14}$$

This function can be evaluated in terms of the complete Elliptic Integrals of the first kind, denoted as $K(m)$ where

$$K(m) = \int_0^{\pi/2}\left(1-m\sin^2(\theta)\right)^{-1/2} d\theta. \tag{15}$$

The Green's function being rewritten as

$$\mathcal{G}(\vec{r}, r_o, z_o) = -\frac{1}{\pi\sqrt{(r+r_o)^2+(z-z_o)^2}}K(m), \qquad m = \frac{4rr_o}{(r+r_o)^2+(z-z_o)^2}. \tag{16}$$

This axisymmetric Green's function can then be again refined in the same manner as demonstrated in Eq. 11 with the form

$$\mathcal{G}_1(\vec{r}, r_o, z_o) = \mathcal{G}(\vec{r}, r_o, z_o) + \mathcal{G}(\vec{r}, r_o, -z_o). \tag{17}$$

Similar to $\mathcal{G}$, $\mathcal{G}_1$ represents a ring source situated at $r = r_o$, $z = z_o$ but located in a semi-infinite space bounded below by the plane $z = 0$.

The task now remains to define the boundary conditions. The bounding surface consists of four parts as outlined in Fig 4a:

1. Jet: an inlet disk of radius R_j located at a given height, Z_j.
2. Free surface: the bounding free streamline surface.
3. Tine stream: a vertical cylinder of radius R_{ts} and height z_s (the vertical distance between the bounding free streamline and the deflector plate) where the flow that does not pass through the deflector plate exits.

4. Deflector: the horizontal deflector plate where flow passes through the ring opening with centroid R_s and total area A_s.

Because of the formulation of the problem as a surface integral, each individual boundary can be evaluated individually, and summed to construct the entire integral as

$$\phi(\vec{r}) = \phi_j(\vec{r}) + \phi_{fs}(\vec{r}) + \phi_{ts}(\vec{r}) + \phi_d(\vec{r}), \tag{18}$$

where $\phi_j(\vec{r})$, $\phi_{fs}(\vec{r})$, $\phi_{ts}(\vec{r})$, and $\phi_d(\vec{r})$ correspond to the integral $\phi(\vec{r})$, as defined in Eq. 9, evaluated on the surface of the inlet jet, free stream, tine stream, and deflector plate, respectively. Because of the inviscid nature of the flow, the distance at which the inlet jet and the tine stream barriers are evaluated is arbitrary. At a sufficient distance from the deflector plate and the vertical axis, respectively, the flow on both of these boundaries converges to some asymptotic behavior.

The impinging jet can be imagined as a circular cylinder of radius R_j with a downward speed U_j extending to infinity. Thus, as $z \to \infty$, $\phi \to -U_j z$. Similarly, the deflector plate with the specified opening governed by R_s and A_s extends so it occupies the entire plane $z = 0$. The jet thickness then approaches 0 as $r \to \infty$. It is worth noting that all analytical solutions for free jet problems described in the literature are posed as infinite domain problems. This has not prevented their use in the study of problems in a finite domain.

It is helpful to construct a global mass balance to quantify how the flow entering through the inlet jet leaves the deflector. The inlet volume flow is dimensionally quantified as $\pi R_j^2 U_j$, or non dimensionally as simply π. A fraction, α, or the flow split, of this flow leaves the domain in the slot stream through one or more holes in the deflector plate. The remaining fraction, $1-\alpha$, is trapped between the surface of the deflector and the ambient air. Because the ambient pressure remains a constant, the speed of the radially moving tine stream must also be U_j. Thus, if we let z denote the thickness of the tine stream, conservation of mass requires that

$$(1-\alpha)\pi R_j^2 U_j = 2\pi r z_s U_j, \tag{19}$$

or non-dimensionally,

$$r z_s = \frac{(1-\alpha)}{2}. \tag{20}$$

The shape of the of the asymptotic streamline leaving the deflector is then a hyperbola whose thickness is determined by the fraction of mass flow passing through the plate or the flow split. The flow split must be determined as a part of the solution to the problem.

Now considering the region $z \gg 1$ far from the deflector plate. The presence of the plate creates a perturbation that retards and expands the jet, deflecting the boundary in the process. The potential at this jet boundary can be represented as

$$\phi_{jet}(r,z) = -z + \Phi(r,z). \tag{21}$$

The appropriate boundary conditions for the pertuirbation potential, $\Phi(r,z)$ are

$$\lim \quad \Phi(r, z \to \infty) = 0 \tag{22}$$

and

$$q^2(1,z) = \left[\left(-1 + \frac{\partial \Phi}{\partial z} \right)^2 + \left(\frac{\partial \Phi}{\partial r} \right)^2 \right] = 1. \tag{23}$$

The first condition requires that the perturbation to the jet flow vanish sufficiently far from the plate while the second arises from the requirement that the pressure and thus the jet speed be uniform at the jet free surface. Neglecting the quadratically small terms the second condition can be simplified to the linearized form

$$\frac{\partial \Phi}{\partial z}(1,z) = 0. \tag{24}$$

Now any solution for $\Phi(r,z)$ can be written as

$$\Phi(r,z) = \sum A_n J_0(\lambda_n r) exp(-\lambda_n z) \tag{25}$$

where A_n are some series of undetermined constants, J_0 are the Bessel functions of order zero and λ_n are a set of eigenvalues corresponding to the Bessel function such that $J_0(\lambda_n) = 0$. Because each subsequent eigenvalue decreases by more than an order of magnitude, only the first term in the series above is important. As a result the asymptotic solution on the jet can now be completed.

The normal velocity is given by

$$v_{jet}(r,z) = -1 - A_0 \lambda_0 J_1(\lambda_0 r) exp(\lambda_0 z) \tag{26}$$

and asymptotic free streamline has the shape

$$r = 1 - A_0 J_1(\lambda_0) exp(-\lambda_0 z). \tag{27}$$

The boundary integral, $\phi_j(\vec{r})$, can now be evaluated at the inlet, a horizontal plane located a non-dimensional distance Z_j above the deflector plate.

$$\phi_j(r,z) = \int_0^{R_j} r_0 (\phi_{jet}(r_0, Z_j) \mathcal{G}_1(\vec{r}, r_0, Z_j) - v_{jet}(r_0, Z_j) \frac{\partial \mathcal{G}_1(\vec{r}, r_0, Z_j)}{\partial z}) dr_0 \tag{28}$$

The chief problem for the general solution to the proposed boundary value problem is selecting an appropriate shape for the free-surface boundary. An approximation of the surface as a hyperbola is a reasonable one for the axisymmetric ring slot case. Using the criteria that the non-dimensional free surface must approach $r = 1$ as $z \to \infty$ the free-surface can be approximated as

$$z = f(r) = A + \frac{B}{r}. \tag{29}$$

where A and B are constants chosen for continuity with the jet and tine stream boundaries.

Assessing the boundary integral, $\phi_{fs}(\vec{r})$, is simplified greatly by the assumption that there is no normal flow to the free-surface. The integral is assessed from $r_0 = 1$, or the radius of the jet, to $r_0 = R_{ts}$, or the arbitrary location of the tine stream boundary, along the curve bounded by the free-surface equation given in Eq. 29. $\phi_{fs}(\vec{r})$ can be written as follows:

$$\phi_{fs}(\vec{r}) = \int_1^{R_{ts}} r_0 \phi(r_0, f(r_0)) \frac{\partial \mathcal{G}_1(\vec{r}, r_0, f(r_0))}{\partial n} dr_0 \tag{30}$$

where $\partial \mathcal{G}_1 / \partial n$ can be found by the following

$$\partial \mathcal{G}_1 / \partial n = \nabla \mathcal{G}_1 \cdot \hat{n} \tag{31}$$

where $\hat{n}$ is the unit normal to the free-surface at any given r_0.

The impact of the next boundary, $\phi_{ts}(\vec{r})$, is now considered. In the region near the plate $r \gg 1$. As $r \to \infty$ the radially expanding jet thins. Since the speed of the jet is fixed by the requirement of constant pressure the limiting form of the solution for large r must be $\phi \to U_j r$. This is not, however, a solution for the fluid potential in this region, but merely the leading term in a descending series. The solution for the velocity potential in this region takes the form

$$\phi_{tine}(r,z) = r + F_1(z)/r + F_2(z)/r^3 + ... \tag{32}$$

Enforcing the boundary condition that $v(r,0) = 0$ gives

$$F_1(z) = -z^2/2! + c \quad \text{and} \quad F_2(z) = z^4/4! + d. \tag{33}$$

Note that this form of the solution restricts its validity to a region of r greater than the radial location of the slot in the deflector plate. The above constants c and d are determined from the requirement that the speed is constant at the free surface. To accomplish this, the equation for the free surface must also be expanded into a descending series in r as

$$z(r) = (1-\alpha)/2r + b/r^3 + ... \tag{34}$$

This introduces another constant, b. The solution for ϕ_{tine} given by Eq. 32 must also be made consistent with the shape of the free surface. The results yield that $b = c = 0$ and $d = -(1-\alpha)^2/4$. This result holds no matter what fraction of the mass flow passes through the plate, subject to the caveat that the domain of applicability lies outside the opening in the plate.

This boundary is evaluated at the arbitrary radius of the plate, $r_0 = R_{ts}$, with the integral spanning $0 < z_0 < z_s$, where z_s is the height of the sheet above the deflector plate given by $z(R_{ts})$ from Eq.34.

$$\phi_{ts}(r,z) = \int_0^{z_s} r_0(\phi_{tine}(R_{ts},z_0)\mathcal{G}_1(\vec{r},R_{ts},z_0) - v_{jet}(R_{ts},z_0)\frac{\partial \mathcal{G}_1(\vec{r},R_{ts},z_0)}{\partial z})dz_0 \tag{35}$$

The final boundary, the deflector, is evaluated at $z_0 = 0$ and spans $0 < r_0 < R_{ts}$. Because of the choice of Green's function, $\partial \mathcal{G}_1/\partial n$ is equal to 0 at all $z = 0$. The term, $\partial\phi/\partial n$ is also equal to 0 at all points where there is no penetration through the boundary. As a result, the integral, $\phi_d(\vec{r})$, can be written as

$$\phi_d(\vec{r}) = \int_0^{R_{ts}} r_0 v(r_0,0)\mathcal{G}_1(\vec{r},r_0,0)dr_0 \tag{36}$$

where $v(r_0)$ is the profile of flow through the ring opening with centroid R_s and total area A_s. This flow profile can be assessed based upon the typical assumptions of 2D slot flow. Using the static pressure at the location of the slot (see Fig. 3b) as calculated from Bernoulli's equation in Eq. 4, a total slot flow, $v(r_0)$, can be determined.

The above integrals can be summed following Eq. 18 to calculate the full potential $\phi(\vec{r})$. The flow split is unknown in any arbitrary axisymmetric geometry. In order to solve for the flow split an iterative process must be performed. First the flow split is estimated, and used to calculate the potential, $\phi(\vec{r})$. Using this calculated potential, pressure on the slot is evaluated, and used to calculate flow through this slot. With this new information, a new flow split is calculated and used to construct new boundary conditions and in turn a new potential. By repeating this process for some given geometric parameters the flow split mandated by the geometry is converged upon. Figure 4b shows a calculated potential flow for the case $R_s = A_s = 1$ with a calculated flow split, $\alpha = 0.62$.

RESULTS

In the previous section, it was mentioned that the axisymmetric model can be used to investigate the impact of the two parameters, slot centroid location, R_s, and total slot area, A_s, which define the ring opening in the deflector plate. The primary quantity of interest in these investigations is the flow split, α. The flow split, while not capable by itself of providing a detailed description of sprinkler spray, is useful as an assessment of sprinkler behavior. Exploring the impact of various parameters on the flow split provides insight into the impact of sprinkler shape on spray behavior.

Figure 5 shows the resulting flow split for a variety of slot centroid locations and slot areas. The model quantifies the effects of increasing slot area and reduced slot centroid (owing to increased pressure at the deflector as in Fig. 3b) on increasing the flow split to the slot stream. The results help to illustrate some of

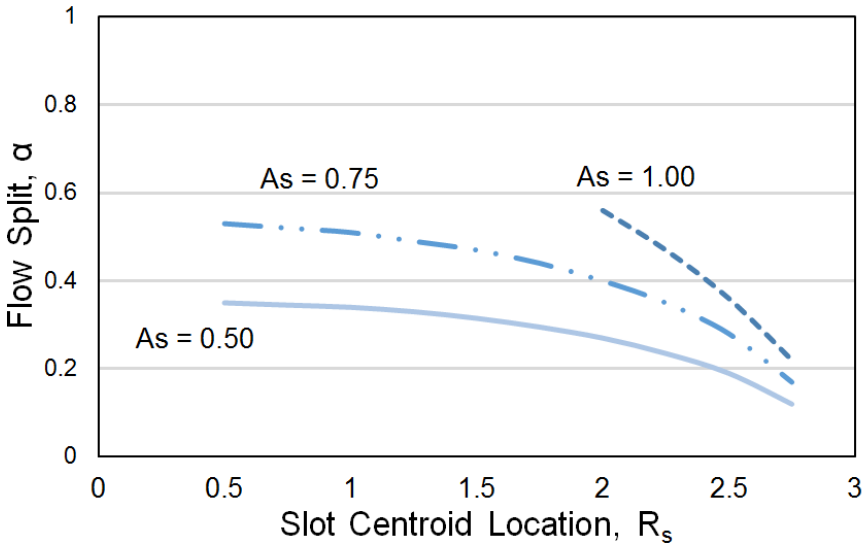

Fig. 5. Calculated flow split from the axisymmetric model.

the meaningful data that can be collected from the axisymmetric model. In addition to the flow split, the thickness and velocity of tine and slot sheets for a given deflector geometry can also be calculated. These can in turn be inputted into the three part sprinkler model as outlined previously in Fig. 1 and used to determine full sprinkler behavior.

An estimate error for the above calculations can be formed by examining the mean deviation from free stream velocity along the streamline was calculated. In the above model, non-dimensional speed along the free-surface should have a constant value of $u^2 + v^2 = 1$. Any slowing or speeding from this velocity is an indication of error. Error can then be written as:

$$\mathcal{E} = \int_1^{R_{ts}} \frac{\sqrt{\left(u(r,f(r))^2 + v(r,f(r))^2 - 1\right)^2}}{\sqrt{1 + \frac{df(r)}{dr}^2}} dr \tag{37}$$

In all cases tested above $\mathcal{E} < 10\%$. The source of this error likely stems from discrepancies in the boundary conditions. The shape of the free-surface may not be precisely a hyperbola and the slot calculations are not perfect representations of flow through a slot. That said, the total error calculated is small, likely less than the error of the physics based models used to calculate sheet breakup and fragment transport [3].

It is important to note that this error only quantifies deviation from an accurate solution of the potential flow equations. There are a number of complications of real flows on real sprinkler heads which would cause calculated results to deviate from true behavior. First, the inviscid and non gravitational assumptions are incorrect for real flows but in flows of the approximate size and speed of sprinkler heads these assumptions are nearly correct. Second, the assumptions made regarding slot behavior break down in the case of particularly large, small, or distant slots. For example, in the case of large or distant slots the hyperbola formulation of the free-surface streamline fails to capture the possibility of flow traveling completely through the slots. Alternatively, in the case of very small slots viscid effects of flow become more important.

It is also important to note the scope of this model. The above general model only accounts for the interaction of an impinging jet with the sprinkler deflector up until the flow leaves the deflector. It does not account for aerodynamic instabilities or air flow effects which dominate the sheet behavior upon leaving the sprinkler head. It can however provide the initialization parameters for these instabilities models and give insight into the poorly understood impact of sprinkler head geometry.

CONCLUSIONS

The mathematical model presented above provides a method for determining the free surface flow field on a perforated deflector plate. By posing the flow impinging on the sprinkler as a potential flow boundary value problem, and applying appropriate boundary conditions and selected Green's functions, the fluid-gas interface location can be determined along with the full deflector flow field. The general nature of this method provides the capability to capture all of the essential features of complex geometries found in typical fire sprinklers.The hypothetical axisymmetric case explored in this study exemplifies the impact of geometric details of the sprinkler (and their associated boundary values) on the deflector flow. Specifically, the impact of slot area and slot centroid radius on the sprinkler head flow split was demonstrated in this study. This flow split is critical as the sheet topology (i.e. location, thickness, and velocity) which governs initial spray details is completely determined from this quantity.

The model developed in this study is capable of capturing this fundamental sheet formation behavior quantitatively with only minimal computational burden. Further work on this problem includes a refinement of the asymptotic boundary conditions on the jet and tine boundaries as well as better selection of free-surface shape. Additional model development will include expansion to capture the periodic geometry (i.e. tines and slots) typical of real fire sprinklers. The sprinkler head deflector flow model is an essential component of a high-fidelity modeling framework capable of completely describing the initial sprinkler spray.

REFERENCES

[1] Marshall, A. " Unraveling Fire Suppression Sprays". *Fire Safety Science* 10, 2011, p. 61-75.

[2] Ren, N., Blum, A., Zheng, Y., Do, C., and Marshall, A., "Quantifying the Initial Spray from Fire Sprinklers" *Fire Safety Science 9*: 2008, p. 503-514.

[3] Ren, N., "Advances in Characterizing Fire Sprinkler Sprays" PhD Thesis, University of Maryland, College Park, USA, 2010.

[4] Hirt, C., and Nichols, B., "Volume of Fluid (VOF) Method for the Dynamics of Free Boundaries" *Journal of Computational Physics*, vol. 39, 1981, p. 201-225.

[5] Lamb, H., *Hydrodynamics*, Sixth Edition, Dover Publications, New York, 1932, p. 94-103.

[6] Batchelor, G.K., *An Introduction to Fluid Dynamics*, Cambridge University Press, 1967, p. 493-506.